THE JOURNAL OF PHYSICAL CHEMISTRY B

ARTICLE

pubs.acs.org/JPCB

Structural, EPR Superhyperfine, and NMR Hyperfine Properties of the Cu−Octarepeat Binding Site in the Prion Protein

Yan Ling,[†] Rahul L. Khade,[†] and Yong Zhang*[,†,‡]

[†]Department of Chemistry and Biochemistry, University of Southern Mississippi, 118 College Drive #5043, Hattiesburg, Mississippi 39406, United States

[‡]Department of Chemistry, Chemical Biology, and Biomedical Engineering, Stevens Institute of Technology, Castle Point on Hudson, Hoboken, New Jersey 07030, United States

Supporting Information

ABSTRACT: Previous experimental and computational investigations show that the copper binding in the prion protein that is involved in a number of neurodegenerative diseases is complicated and the exact binding structures remain to be determined. To facilitate structural investigation in this field, we report a quantum chemical investigation of structural, EPR superhyperfine, and NMR hyperfine properties of various copper complexes of the octarepeat domain, which has several copies of highly conserved amino acid sequence of PHGGGWGQ. The predicted metal−ligand bond lengths of the X-ray structure of CuHGGGW, involving the central five residues in this domain, from the best method examined here, have a mean absolute deviation (MAD) of 0.030 Å, basically the same as found with experimental errors of various metal complexes. Prior controversial results regarding water coordination were resolved here with a more extensive computational investigation on 10 models with various water molecules and sequences (both HGGGW and PHGGGWGQ), which are consistent with the experimental reports. Experimental EPR superhyperfine constants are accurately reproduced with a MAD of 0.95 MHz. Results here suggest that the NMR hyperfine shifts which can be readily measured in NMR experiments and accurately predicted in quantum chemical calculations can provide more extensive and more sensitive structural probes than those from the current EPR studies. These results will be helpful for future experimental and computational investigations of the copper binding structures of the prion protein as well as other related systems.

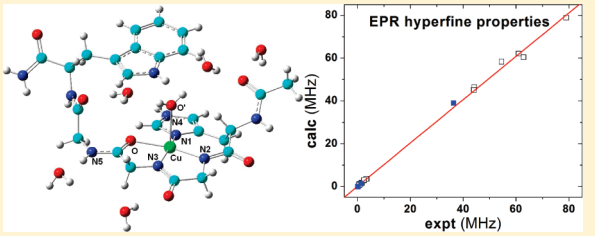

INTRODUCTION

Prions are the proteinaceous infectious particles responsible for mad cow disease, scrapie in sheep and goats, chronic wasting disease in deer and elk, and the human diseases kuru and new variant Creutzfeldt−Jakob disease (nvCJD), which are collectively referred to as transmissible spongiform encephalopathies (TSEs).[1,2] The prion protein is a normal component of many body tissues and is found at high levels in the central nervous system. However, the normal cellular form (PrP^{C}) may be transformed into the misfolded scrapie form (PrP^{Sc}), which acts as a template to convert other normal PrP^{C} into PrP^{Sc}. This propagates the misfolded form and generates amyloid fibrils, which leads to lethal neurological disorders. More and more experimental studies show that copper can bind with the prion protein in various sites.[3−14] Possible functional roles of copper binding in the prion protein include superoxide dismutase-like function,[15] transmembrane copper transporter,[5] copper buffer to sequester excess metal ion at the plasma membrane,[16] and promotion of fibril formation.[11] The most extensively investigated site is the octarepeat domain, which has a highly conserved amino acid sequence of PHGGGWGQ and has four copies in residues 60−91. One of the significant discoveries is an X-ray structure of the copper bound HGGGW unit,[5] which contains the central five amino acids in the octarepeat domain as well as six solvent water molecules (one of them is coordinated to Cu). However, even for the octarepeat site, a number of copper binding modes or geometries were proposed[3−8] from different experimental studies. These results suggest that copper binding in the prion protein is complicated and may be affected by different experimental conditions. In addition, experimental investigations indicate that the binding structure may also be influenced by sequence specificity.[4,10−14] Therefore, the exact structures of the copper binding sites in the prion protein remain to be determined.[3,5,11,15,16]

To help understand copper binding in the octarepeat domain, many computational investigations have been reported, which involve different structural models including CuHG,[17] $CuHGGG\cdot xH_2O$ (x = 0, 1, 3, 6),[17−22] $CuHGGGW\cdot xH_2O$ (x = 0, 1, 3, 6),[18,19,21−23] $CuPHGGGWGQ\cdot 5H_2O$,[24] and CuPrP(61−84).[21] Results suggest that both the sequence specificity and the number of solvent molecules (H_2O) have effects on the structures. For instance, recent computational studies of

Received: December 15, 2010
Revised: January 26, 2011
Published: February 28, 2011

CuHGGGW·0H_2O and CuHGGGW·1H_2O indicate that copper has a strong tendency to form the square planar geometry to prevent the addition of water molecule in its coordination sphere.[23] Molecular dynamics simulations with the CuPHGGGWGQ·5H_2O model and CuHGGGW·1H_2O showed that the axial water is very labile.[22,24] These results are in support of the recent ESI-MS and EXAFS experimental investigations that the water molecule may not bind in the axial position in the octarepeat region,[6,25] contrary to the X-ray crystal structure of the HGGGW fragment.[5] However, recent calculations of using the CuHGGGW·3H_2O model did show stable coordination of the axial water.[19]

These experimental and computational results call for more extensive investigations of the copper bindings in the prion protein. Spectroscopic techniques usually can provide valuable observable information to probe the structures. Due to the intrinsic quantitative structure-observable relationships (QSOR),[26] high accuracy quantum chemical investigations of experimental spectroscopic observable properties and candidate structural models were found to be useful in quantitative structure refinement and/or determination for metals sites in biomolecules.[27−34] These approaches with various types of QSORs were referred to as integrated quantum mechanics and spectroscopy (QM/S) techniques. It should be noted that EPR and NMR techniques have been extensively used to investigate the copper complexes of prion models,[4,5,7,8,10−13] since Cu(II) is paramagnetic in nature. Computational investigations have also been reported for some EPR properties of the copper binding site in the octarepeat domain.[19,20] However, there are no experimental or computational investigations of the NMR hyperfine properties. As a matter of fact, recent developments have even enabled experimental solid-state NMR techniques to be valuable tools in investigating various solid systems, in particular the disordered ones that include the disease or fibrillar forms of some prion proteins.[35,36] Predictions of experimental solid-state NMR hyperfine shifts in paramagnetic metal complexes, including a Cu(II) amino acid complex,[37,38] have achieved an accuracy with the theory-versus-experiment correlation coefficient $R^2 = 0.96$, and calculations of the solution NMR hyperfine shifts of a number of metallobiomolecules and models including copper-containing proteins have also been found to be accurate with $R^2 = 0.99$.[32,39,40] These computational studies have assisted in many structural investigations.

To facilitate structural investigation of the copper bindings in the prion protein, in this paper, we report a quantum chemical investigation of structural, EPR superhyperfine, and NMR hyperfine properties of various copper complexes of the octarepeat domain. Results indicate that (1) the predicted metal−ligand bond lengths can have a mean absolute deviation (MAD) of 0.030 Å, basically the same as found with experimental errors of various metal complexes;[41] (2) the prior controversial results regarding the water coordination can be resolved here with a more extensive computational investigation on models with various water molecules and sequences, which are consistent with the experimental reports; (3) EPR superhyperfine constants can be predicted with a MAD of 0.95 MHz, which, however, are not sensitive to some structural variations; and (4) NMR hyperfine shifts can provide more extensive and more sensitive structural probes than those from the current EPR studies.

COMPUTATIONAL DETAILS

In order to find an appropriate level of method to best reproduce experimental geometric results, the first series of calculations were carried out on the X-ray crystal structure of CuHGGGW,[5] as shown in Figure 1, using eight different geometry optimization methods. Due to the excellent performance of the hybrid Hartree−Fock and density functional theory (HF-DFT) method mPW1PW91[42,43] in previous structural investigations of various types of transition metal complexes,[44−47] it was examined here with five different basis sets to form method 1 through method 5. Method 1 uses a uniform double-ζ valence split basis set 6-31G(d). In comparison, method 2 has one set of diffuse functions added for the basis set used for Cu and first coordination shell atoms, while the rest part of the system is still treated with 6-31G(d). This basis set scheme is noted as 6-31+G(d)|6-31G(d) in this work. Method 3, however, introduces an additional set of d functions to Cu and first coordination shell atoms, compared to method 1. Therefore, it uses the following scheme: 6-31G(2d)|6-31G(d). Method 4 was used to examine the effect of triple-ζ basis set in comparison to that used in method 3, so the basis set is 6-311G(2d)|6-31G(d). Method 5 has both additional d functions and diffuse functions for Cu and its directly bonded atoms, as 6-31+G(2d)|6-31G(d). To examine the effect of using other percentage of HF exchange in the hydrid HF-DFT method, method 6 (BHandHLYP/6-31+G(d)|6-31G(d)) was used. This hybrid functional has 50% HF exchange and 50% Becke exchange[48] together with the LYP correlation functional,[49] in contrast with the 25% HF exchange used in mPW1PW91 method. Because recently the pure DFT method SVWN using the Slater type or local spin density exchange[50] and VWN correlation functional[51] was found to yield excellent predictions of bond lengths in many metal complexes except for Cu complexes,[41] this method was also tested here with two different basis sets to form method 7, SVWN/6-31+G(d)|6-31G(d), and method 8, SVWN/6-31+G(d).

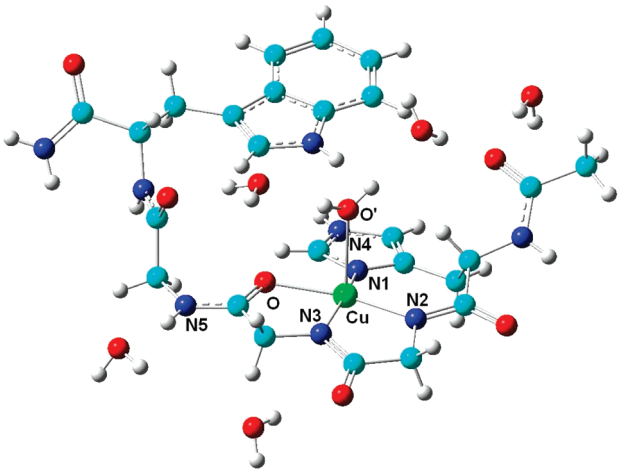

Figure 1. X-ray structure of CuHGGGW from ref 5. Color schemes: Cu, green; O, red; N, blue; C, cyan; H, gray.

The second series of calculations were performed to evaluate the EPR superhyperfine constants in ten different models for the octarepeat Cu-binding site in the prion protein to examine the sensitivity of the structural dependence of such spectroscopic properties. Four models were built on the basis of the CuHGGGW original X-ray structure.[5] **1** is exactly the same as the unit cell, as shown in Figure 1, and is noted as CuHGGGW-complete. Compared to **1**, **2** has no central water molecule, **3** does not have any water molecules except for the central one, and

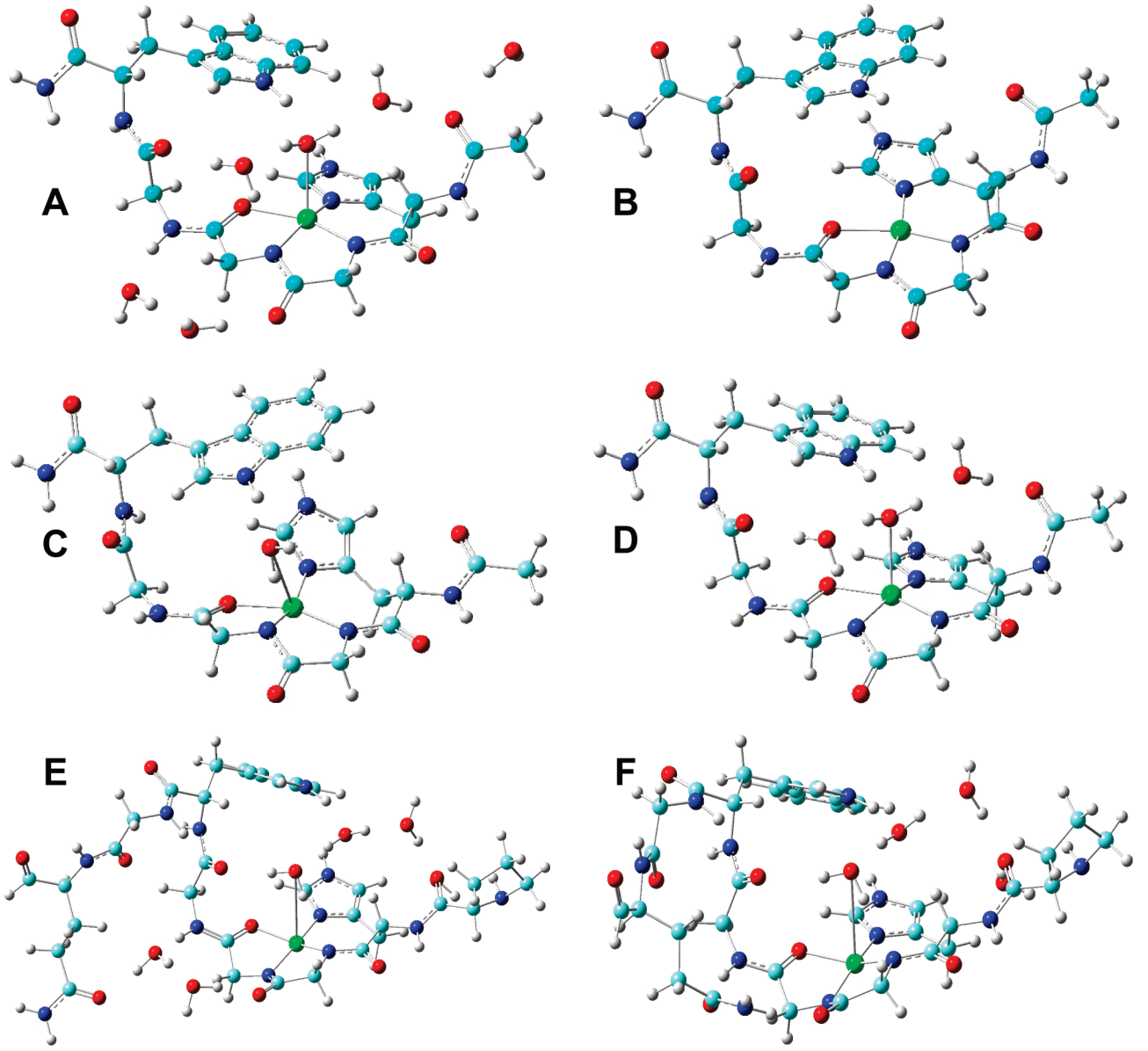

Figure 2. Optimized molecular structures: (A) **5**; (B) **6**; (C) **7**; (D) **8**; (E) **9**; (F) **10**.

in **4** the Trp residue is replaced by a hydrogen atom. To further examine the effect of water molecules (which are also good probes of hydrogen bondings) in CuHGGGW and sequence effect, six optimized models were used. **5** is the fully optimized structure of **1**; see Figure 2A. **6** is an optimized CuHGGGW model without any water molecules (Figure 2B). As shown in Figure 2, C and D, **7** and **8** are optimized CuHGGGW models with one and three central water molecules, respectively. **9** has the full eight residues (PHGGGWGQ) in the octarepeat region, instead of just HGGGW as in **5**; see Figure 2E. In **10**, the two water molecules originally in the X-ray structure of CuHGGGW that prevents the formation of intramolecular hydrogen bonds between the newly added GQ residues and the original GG part of the HGGGW section were removed, as shown in Figure 2F. The optimized coordinates for **5**−**10** are listed in Tables S1−S6 in the Supporting Information.

The isotropic superhyperfine coupling constant (A) of a given nucleus can be computed from the spin density at that nucleus ($\rho_{\alpha\beta}$), using the relation[28]

$$A = \frac{8\pi}{3}\hbar\gamma_n g_e \beta_e \rho_{\alpha\beta} \quad (1)$$

where $\hbar$ is Planck's constant divided by 2π, γ_n is the nuclear gyromagnetic ratio, g_e is the free electron g-factor, and β_e is the Bohr magneton.

In addition, NMR hyperfine shifts calculations were also carried out on these 10 structural models. The NMR hyperfine shift is computed from the Fermi contact contribution as follows with the pseudocontact term neglected as usual[37,38]

$$\delta_{hf} = m(S+1)\rho_{\alpha\beta}/T \quad (2)$$

where S is the spin state of the system, T the temperature, and m is a collection of physical constants and is equal to 2.35×10^7 ppm K au^{-1}.[37,38] Here, the NMR hyperfine shifts of the copper binding models were all evaluated at room temperature 298 K.

dx.doi.org/10.1021/jp1119298 |J. Phys. Chem. B 2011, 115, 2663–2670

Table 1. Experimental and Optimized Structural Parameters of CuHGGGW by Different Methods[a]

method	R_{CuN1} (Å)	R_{CuN2} (Å)	R_{CuN3} (Å)	R_{CuO} (Å)	$R_{CuO'}$ (Å)	MAD1 (Å)	∠N1−Cu−N2 (deg)	∠N1−Cu−O (deg)	∠N2−Cu−N3 (deg)	∠N3− Cu−O (deg)	MAD2 (deg)
X-ray	1.990	1.996	1.921	2.066	2.380		106.3	91.0	82.1	80.4	
1	2.007	1.945	1.898	2.193	2.269	0.068	102.9	90.6	83.0	78.3	1.7
2	2.003	1.948	1.917	2.161	2.341	0.040	104.6	89.5	83.4	78.6	1.6
3	1.997	1.944	1.892	2.157	2.301	0.051	103.2	90.5	83.1	79.0	1.5
4	2.001	1.945	1.897	2.193	2.293	0.060	103.1	90.5	83.3	78.4	1.7
5	1.996	1.947	1.910	2.138	2.366	0.030	104.9	89.7	83.4	78.9	1.4
6	2.025	1.984	1.906	2.189	2.285	0.056	104.9	90.5	82.9	78.7	1.1
7	1.911	1.928	1.859	2.153	2.159	0.103	104.0	89.6	82.2	80.3	1.0
8	1.921	1.960	1.873	2.130	2.300	0.060	106.2	90.5	81.6	80.5	0.3

[a] Method 1: mPW1PW91/6-31G(d). Method 2: mPW1PW91/6-31+G(d)|6-31G(d). Method 3: mPW1PW91/6-31G(2d)|6-31G(d). Method 4: mPW1PW91/6-311G(2d)|6-31G(d). Method 5: mPW1PW91/6-31+G(2d)|6-31G(d). Method 6: BHandHLYP/6-31+G(d)|6-31G(d). Method 7: SVWN/6-31+G(d)|6-31G(d). Method 8: SVWN/6-31+G(d). See text for details. X-ray results are from ref 5.

The hybrid HF-DFT method B3LYP[49,52] together with a Wachters' basis (62111111/3311111/3111) for Cu,[53] 6-311G-(d) for all the other heavy atoms and 6-31G(d) for hydrogens were used to calculate both EPR and NMR properties, since this approach was found to enable accurate predictions of such spectroscopic properties in various types of metal complexes including a copper amino acid complex.[37,38,40] These calculations together with geometry optimizations were all done using the Gaussian 03 programs.[54]

RESULTS AND DISCUSSION

Structural Properties. Since the X-ray structure of CuHGGGW is the only one that is available for any copper binding sites of the proteins involved in the neurodegenerative diseases, it is used as a benchmark here to find an appropriate level of computational method for structural prediction. Previous computational studies indicate that the quality of the optimized geometries of Cu−octarepeat models has a clear dependence on the methods used.[17−21,23,24] Here, our goal is to find one method that could result in basically the same average error as with the experimental measurements and also has a reasonable computational cost. Prior investigations indicate that the average error of experimental metal−ligand bond lengths in a number of different metal complexes is ca. 0.03 Å.[41]

A number of computational methods were examined here, as shown in Table 1. We began the investigation with the use of the hybrid HF-DFT method mPW1PW91, since it was found to yield excellent geometries in structural investigations of various types of transition metal complexes.[44−47] As seen from Table 1, the mean absolution deviation of the five copper coordination bonds (MAD1) of the mPW1PW91/6-31G(d) calculation is 0.068 Å, which is ca. twice the experimental error. The MADs were decreased by 0.028 and 0.017 Å, respectively, upon using either one set of diffuse function (method 2) or an extra set of d functions (method 3) in Cu and first coordination shell atoms. In contrast, the use of the relatively large scale triple-ζ basis together with an extra set of d functions (method 4) only slightly improved the performance by 0.008 Å. Therefore, the next investigation is to examine the combined effect from methods 2 and 3, i.e., method 5. As shown in Table 1, now the MAD1 is 0.030 Å, basically our targeted value. We also did a few more calculations to see if the errors could be further reduced. For instance, method 6 involves a hybrid HF-DFT method (BHandHLYP) that has more HF exchange (50%) compared to that in mPW1PW91 (25%). However, its results are inferior to those from using mPW1PW91 with the same basis set scheme. On the other hand, the pure DFT calculations without any HF exchange contributions were also done, methods 7 and 8 in Table 1, which involves the use of SVWN method that was found to yield excellent predictions of bond lengths in many metal complexes.[41] However, this method has not been examined for Cu complexes yet. Now, for CuHGGGW, with the same level of basis set, the use of SVWN in Method 7 results in a MAD1 is ca. 2.5 times larger than that from using mPW1PW91 (method 2). The use of even larger basis set in method 8 still could not improve the performance comparable to method 5 with an overall smaller set of basis functions. Regarding the bond angle predictions, the mean absolute deviations (MAD2) are all close to one degree, a reasonably good accuracy. So, based on these results, method 5 which has basically the same error as found with many experiments was used to optimize the copper binding models in this work.

Altogether, six optimized structural models of the octarepeat site (**5**−**10**) were investigated, involving different numbers of water molecules and sequences. The optimized model of the complete unit cell of the X-ray structure (**5**) results in the smallest deviations in geometric parameters (see Table 2) which suggests that the use of different water network and sequences may affect the final geometries. Therefore, caution is needed in structural investigations of the copper bindings in the prion protein. The use of **6** without any water molecules only leads to a small increase in geometric deviations compared to those for **5**; e.g., MAD1 is increased by 0.017 Å. With one central water molecule initially put in the axial position of the X-ray structure (**7**), this water molecule eventually moves away from the copper center with a Cu···O distance of 3.561 Å after the optimization, as shown in Figure 2. So, our calculations of the CuHGGGW·0H_2O and CuHGGGW·1H_2O models are consistent with previous reports on the same models, which showed that copper is not in favor of binding the water molecule in the axial position of this CuHGGGW system.[23] However, as shown in Figure 2 and Table 2, the use of three central water molecules almost reproduces the copper coordination geometry, since the MAD1 is only enhanced by 0.007 Å compared to that of the optimized complete experimental model **5**. This result is also consistent with recent calculations using the same models.[19] Therefore, our results of the most extensive investigation of the

Table 2. Experimental and Optimized Structural Parameters of Cu−Octarepeat Binding Models[a]

model	R_{CuN1} (Å)	R_{CuN2} (Å)	R_{CuN3} (Å)	R_{CuO} (Å)	$R_{CuO'}$ (Å)	MAD1 (Å)	∠N1−Cu−N2 (deg)	∠N1−Cu−O (deg)	∠N2−Cu−N3 (deg)	∠N3−Cu−O (deg)	MAD2 (deg)
X-ray	1.990	1.996	1.921	2.066	2.380		106.3	91.0	82.1	80.4	
5	1.996	1.947	1.910	2.138	2.366	0.030	104.9	89.7	83.4	78.9	1.4
6	1.956	1.934	1.865	2.103	−	0.047	106.5	88.8	84.6	80.1	1.3
7	1.938	1.933	1.899	2.051	3.561	0.267	106.7	89.4	85.9	81.7	1.8
8	2.003	1.937	1.921	2.157	2.358	0.037	104.8	88.8	84.5	78.5	2.0
9	1.931	1.955	1.881	2.046	3.313	0.219	105.6	90.1	85.5	82.2	1.7
10	1.931	1.956	1.872	2.071	3.270	0.209	106.7	91.6	85.6	83.0	1.8

[a] X-ray results are from ref 5.

Table 3. Experimental and Computed EPR Parameters of Cu−Octarepeat Binding Models

		model	A_N (MHz)	A_H (MHz)	A_{N4} (MHz)	A_{N5} (MHz)
		expt[a]	36.4	<0.2		1.41
X-ray	**1**	CuHGGGW-complete	38.9	−0.15	1.65	1.36
	2	CuHGGGW-no central water	39.5	−	1.60	1.37
	3	CuHGGGW-no other water	38.4	−0.10	1.59	1.92
	4	CuHGGGW-no Trp	38.6	−0.11	1.47	1.16
optimized	**5**	CuHGGGW-complete	38.6	−0.01	1.80	1.12
	6	CuHGGGW-0 water	39.3	−	1.77	1.90
	7	CuHGGGW-1 central water	35.2	0.02	1.99	1.65
	8	CuHGGGW-3 central water	36.8	0.06	1.76	1.64
	9	CuPHGGGWGQ-complete water	35.7	0.02	1.79	1.27
	10	CuPHGGGWGQ-partial water	32.9	0.11	1.60	1.25

[a] Experimental results are from ref 5.

water network (CuHGGGW·xH$_2$O, x = 0, 1, 3, 6) indicate that the controversial results in previous studies are due to the effect of different water networks. Since in the real prion protein it is the full PHGGGWGQ sequence and not just the HGGGW fragment involved in copper binding, we next investigated a couple of CuPHGGGWGQ models. **9** has the full eight residues (PHGGGWGQ) in the octarepeat region, with the proline, the last glycine, and glutamine added on **5**; see Figure 2E. This results in a dramatic increase in MAD1 by 0.189 Å, with the most significant change being that for the central water molecule. Now in **9** this water molecule again moves out of the coordination shell with a Cu···O distance of 3.313 Å. In **10**, formation of intramolecular hydrogen bonds between the newly added GQ residues and the original GG part of the HGGGW section were observed once the two water molecules hydrogen bonded to the GG part of the CuHGGGW X-ray structure were removed, as shown in Figure 2F. But the overall coordination geometry is similar to that in **9**, since the MAD1 for **10** differs by 0.01 Å from that of **9**. Again, the central water molecule is not bonded to Cu, as the Cu···O distance is still as long as 3.270 Å. So, these results suggest that the axial water molecule is indeed labile, as observed in recent experimental EXAFS and ES-MSI and computational investigations.[6,22−25]

EPR Superhyperfine Constants. EPR superhyperfine constants provide atomic level responses, which may be used to probe many atoms in a molecule of interest. As shown in Table 2, previous EPR experiments[5] yielded a single large isotropic superhyperfine constant (36.4 MHz) for the three directly bonded nitrogen atoms (N1, N2, N3 in Figure 1), a small superhyperfine constant (1.41 MHz) for N5 (the amide nitrogen in the third glycine of the HGGGW fragment), and an even smaller superhyperfine constant (<0.2 MHz) for the hydrogen atoms in the central directly bonded water molecule. These frozen solution EPR results were reproduced well in the calculation using the unit cell of the experimental CuHGGGW X-ray structure, model **1**, as seen from Table 3. This indicates that structural model **1** is compatible with the EPR experiment. As illustrated in Figure 3, the results are basically in the same theory-versus-experiment regression line when compared with the ligand EPR superhyperfine constants calculated in other metal complexes[37] using the same method. The overall correlation coefficient R^2 now is 0.998 with a standard deviation (SD) of 0.97 MHz. The predicted A_N value from our calculation is also similar to the values reported previously using relatively smaller models as CuHGGG·6H$_2$O[20] and CuHGGGW·3H$_2$O[19] with the same B3LYP method. This suggests that either these EPR superhyperfine constants are not sensitive to structural variations in the copper binding site of the octarepeat region of the prion protein or structural variations from using these models may be too small to result in significant differences, so these EPR results alone may not be sufficient to determine the structure of the copper binding site. To further examine the structural sensitivity of the EPR superhyperfine constants, we performed two sets of comparisons.

The first set of calculations was done with the X-ray structure with some parts modified. It is interesting to note that, with the same X-ray geometry, the differences of the predicted EPR superhyperfine constants (A_N, A_H, A_{N4}, and A_{N5}) from using different water molecules are all small; Table 3 for results of models **1**−**3**, with 6, 5, and 4 water molecules, respectively. The

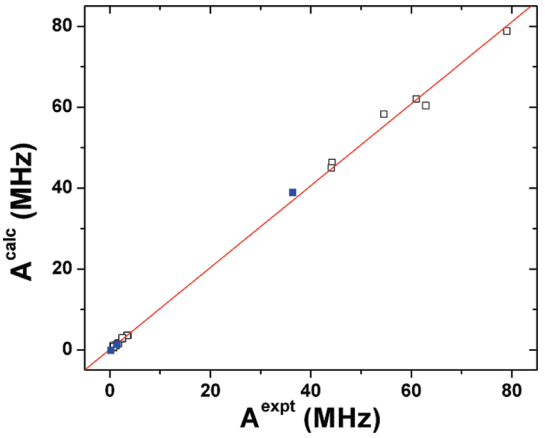

Figure 3. Plot of the predicted versus experimental hyperfine couplings. The blue data points are from this work and hollow square points are from ref 37 using the same method.

largest difference is for A_N between **2** and **3**, of 1.1 MHz, which is close to the SD of the calculations. These results are consistent with those from a previous report using a smaller model as CuHGGG with 0, 3, and 6 water molecules.[20] Since our models have a Trp residue compared to these previous calculations, model **4** which keeps all water molecules but replaces the Trp residue with a hydrogen atom was also investigated here. Again, it shows negligible differences; see Table 3. These results indicate that even the directly bonded axial water molecule and its hydrogen-bonded Trp residue play little role in determining experimental EPR superhyperfine results.

To see if this conclusion could be an artifact of the use of modified X-ray models, additional calculations were done with geometry-optimized ones (**5**−**10**). Among all the optimized models of different water molecules and sequences investigated here, it is the optimized model of the complete unit cell of the X-ray structure (**5**) that results in the smallest deviations in EPR superhyperfine constants (Table 3), compared to the experimental data. This coincides with the fact that this model also has the smallest geometric deviations. As discussed in the previous section, both the water network and sequence can affect the optimized geometries. Such structural variations result in the most significant differences in the EPR superhyperfine coupling constant A_N, as shown in Table 3. For instance, models **7**, **9**, and **10** have the largest structural changes compared to the X-ray model, and the A_N values also show the largest deviations. Such structural sensitivity is due to the fact that this property is for the directly bonded nitrogen atoms. In contrast, the EPR superhyperfine constants of the distant nitrogen atoms N4 and N5 have little variation upon using different models. The EPR superhyperfine constants of the water hydrogen atoms are always negligible (from −0.15 to 0.11 MHz), even in the stably coordinated models (Table 3). However, this may not be surprising, since previous investigations show that, with different numbers of water molecules, the singly occupied molecular orbitals are basically the same, which involves Cu $d_{x^2-y^2}$ orbital and orbitals of equatorial ligands.[20] Therefore, superhyperfine constants of atoms in the axial positions are small.

These results suggest that, except for A_N, the other experimentally measured EPR superhyperfine coupling constants are of little help in investigating different structural models. Even for A_N, for models **7** and **9** which have the largest MAD1 with respect to the X-ray structure; it only changes ca. 3 MHz or 8% compared to that in the X-ray model.

NMR Hyperfine Shifts. In order to find more sensitive structural probes, we next investigated the NMR properties of the copper−octarepeat binding models. For paramagnetic systems such as the copper prion protein models investigated here, the NMR hyperfine shifts should be valuable probes, as they are also proportional to the spin densities as with the superhyperfine coupling constants measured in EPR experiments (see eqs 1 and 2). Moreover, the NMR hyperfine shift in the unit of ppm is much larger than the corresponding EPR superhyperfine constant in the unit of MHz. For instance, N5 has a predicted EPR superhyperfine constant of 1.36 MHz in the complete X-ray model (which is in excellent agreement with the experimental value of 1.41 MHz),[5] corresponding to a predicted 497 ppm for the NMR hyperfine shift at room temperature 298 K. This makes the NMR technique more appealing in measuring small changes. Our group recently reported the first computational investigation of experimental solid-state ^{13}C and ^{1}H NMR hyperfine shifts in paramagnetic metal complexes including a Cu(II) amino acid complex,[37,38] with the theory-versus-experiment correlation coefficient R^2 = 0.96, and our calculations of the solution NMR hyperfine shifts of a number of metallobiomolecules and models including copper-containing proteins have also been found to be accurate with R^2 = 0.99.[32,39,40] On such a basis, we performed two series of computational investigations of the NMR hyperfine shifts for the copper binding models **1**−**10**. Here, we focus on solid-state NMR results, since they may be helpful to determine the metal binding structures in the disease or fibrillar forms of the prion proteins, as solid-state NMR techniques were recently proved to be powerful in structure determination of such forms of prion proteins.[35,36]

The first set of calculations was done with different models of the X-ray structure (**1**−**4**). As shown in Table 4, there are a number of carbon atoms that have significant differences in ^{13}C NMR hyperfine shifts for models with truncated water molecules or the Trp residue (**2**, **3**, **4**) compared to the complete X-ray model **1**. The differences that are larger than the SD of the calculations are highlighted in bold. As the singly occupied molecular orbitals in these models are basically the same, involving Cu $d_{x^2-y^2}$ orbital and orbitals of equatorial ligands,[20] the significant changes in NMR hyperfine shifts from model **1** to models **2**−**4** also occur in the equatorial plane. Since models **2**−**4** all involve deletion of some groups with respect to **1**, such changes reduce the size of the system that can accept delocalized spin densities, which consequently increase the spin densities and the corresponding NMR hyperfine shifts of the four coordinating atoms N1, N2, N3, and O (see Figure 1) shown in Table 4. It is also interesting to note that the average changes of the NMR hyperfine shifts for these four coordinating atoms in models **2**−**4** with respect to those in **1** have the following order: 497 ppm (in **3**) > 234 ppm (in **2**) > 123 ppm (in **4**), which is consistent with the extents of structural modifications in these models: with respect to model **1**, **3** involves the deletion of five water molecules, **2** has only one axial water molecule deleted, and **4** also has one group (Trp) removed and this Trp unit is even further away than the axial water molecule. Changes of NMR hyperfine shifts of nearby atoms also follow this pattern. For instance, there are three, four, and two significant changes of ^{13}C NMR hyperfine shifts (bold numbers in Table 4) in models **2**, **3**, and **4**, respectively, which again have the same trend of **3** > **2** > **4** as with structural differences.Overall, these calculations indicate that a number of

Table 4. Computed NMR Hyperfine Shifts of X-ray Models (ppm)

model	1	2, Δ^a	3, Δ^a	4, Δ^a
N1	8477	67	360	205
N2	19312	442	555	174
N3	14862	407	785	51
O	9191	20	289	64
His Cα	−47	**-31**	−22	−9
His Cβ	−22	0	−2	5
His Cγ	−91	9	−4	−7
His Cδ	198	1	−7	−18
His Cε	648	20	24	**51**
His C′	699	21	**80**	7
Gly1 Cα	−187	22	**69**	−5
Gly1 C′	−722	**-51**	**-52**	−19
Gly2 Cα	−148	**-34**	**41**	**-38**
Gly2 C′	−258	−14	−9	11

[a] Difference from that in model **1**.

Table 5. Computed NMR Hyperfine Shifts of Optimized Models (ppm)

model	5	6, Δ^a	7, Δ^a	8, Δ^a	9, Δ^a	10, Δ^a
His Cα	−41	**-44**	**-54**	−9	**-41**	**-46**
His Cβ	6	−4	−14	−5	**-57**	**-63**
His Cγ	−70	**-69**	**-88**	−26	51	25
His Cδ	212	−17	24	−14	66	**45**
His Cε	603	**185**	**260**	**41**	−1	**-39**
His C′	833	**114**	−20	**143**	−302	**-386**
Gly1 Cα	−89	**51**	**92**	**122**	−157	**-194**
Gly1 C′	−680	**-80**	−21	**-37**	−34	**-64**
Gly2 Cα	−187	**160**	**-159**	**96**	−168	**-211**
Gly2 C′	−239	−4	5	25	−25	**54**

[a] Difference from that in model **5**.

significant differences can be readily measured in NMR experiments to sensitively probe different structural features. This is in contrast with basically no significant differences in all the EPR superhyperfine constants from using the same models, discussed above, as shown in Table 3.

The second set of calculations was done with geometry optimized model (**5**−**10**). As shown in Table 5, the ^{13}C NMR hyperfine shift results here show even more extensive significant differences, indicating structural sensitivities of these NMR spectroscopic probes. From these data, it can be seen that ^{13}C NMR hyperfine shifts in model **8** have the smallest differences compared to those in **5**, which is consistent with the structural results that model **8** is most similar to **5** among all models investigated here. Models **7**, **9**, and **10** which have relatively larger structural changes compared to **6** and **8** also have relatively more significant NMR hyperfine shift differences. For instance, the largest changes in **7**, **9**, and **10** are 260, −302, and −386 ppm, respectively, which are greater than 185 and 143 ppm, the corresponding largest changes in **6** and **8**. These results clearly show that NMR techniques may be useful in structural investigations of copper bindings in the prion protein and the combined use of experimental NMR data and quantum chemical studies may help elucidate the binding structures.

CONCLUSIONS

The results we have described above are of interest for a number of reasons. First, the methodological studies indicate that the mPW1PW91/6-31+G(2d)|6-31G(d) calculation is able to reproduce the experimental geometry with a mean absolute deviation of 0.030 Å for the coordination bond lengths, which is basically the same as the average experimental error for many metal complexes.[41] The mean absolute deviation of bond angles is about 1°. Second, our results indicate that the controversial results in previous studies regarding water coordination in CuHGGGW models are due to the effect of the use of different water networks. Third, the quantum chemical investigation of a couple of CuPHGGGWGQ models here indicate that the axial water molecule is indeed labile, as observed in recent experimental EXAFS and ES-MSI and computational investigations.[6,22−25] Fourth, EPR superhyperfine constants can be predicted with a MAD of 0.95 MHz. However, they are not sensitive to some structural variations. Fifth, the NMR hyperfine shifts can provide more extensive and more sensitive structural probes than those from the current EPR studies. Taken together, these results should facilitate the use of quantum chemical investigations and spectroscopic studies for the structural characterization of the copper binding sites in the prion protein and other related systems.

ASSOCIATED CONTENT

Supporting Information. Coordinates of the optimized models **5**−**10** (Tables S1−S6). This material is available free of charge via the Internet at http://pubs.acs.org.

ACKNOWLEDGMENT

This work was supported in part by the NSF EPSCoR grant OIA-0556308, the Summer Faculty Research Grant from the University of Southern Mississippi, and the start-up fund from Stevens Institute of Technology. Y.Z. thanks Rebecca Weber for participation in the early stage of this project. We are also grateful to the Mississippi Center of Supercomputing Research and USM Vislab for generous use of their computing facilities.

REFERENCES

(1) Prusiner, S. B. *Science* **1997**, *278*, 245–251.
(2) Prusiner, S. B. *Proc. Natl. Acad. Sci. U.S.A.* **1998**, *95*, 13363–13383.
(3) Millhauser, G. L. *Acc. Chem. Res.* **2004**, *37*, 79–85.
(4) Aronoff-Spencer, E.; Burns, C. S.; Avdievich, N. I.; Gerfen, G. J.; Peisach, J.; Antholine, W. E.; Ball, H. L.; Cohen, F. E.; Prusiner, S. B.; Millhauser, G. L. *Biochemistry* **2000**, *39*, 13760–13771.
(5) Burns, C. S.; Aronoff-Spencer, E.; Dunham, C. M.; Lario, P.; Avdievich, N. I.; Antholine, W. E.; Olmstead, M. M.; Vrielink, A.; Gerfen, G. J.; Peisach, J.; Scott, W. G.; Millhauser, G. L. *Biochemistry* **2002**, *41*, 3991–4001.
(6) Bonomo, R. P.; Cucinotta, V.; Giuffrida, A.; Impellizzeri, G.; Magri, A.; Pappalardo, G.; Rizzarelli, E.; Santoro, A. M.; Tabbi, G.; Vagliasindi, L. I. *Dalton Trans.* **2005**, 150–158.
(7) Mentler, M.; Weiss, A.; Grantner, K.; Pino, P. d.; Deluca, D.; Fiori, S.; Renner, C.; Klaucke, W. M.; Moroder, L.; Bertsch, U. K., H. A.; Tavan, P.; Parak, F. G. *Eur. Biophys. J.* **2005**, *34*, 97–112.
(8) Chattopadhyay, M.; Walter, E. D.; Newell, D. J.; Jackson, P. J.; Aronoff-Spencer, E.; Peisach, J.; Gerfen, G. J.; Bennett, B.; Antholine, W. E.; Millhauser, G. L. *J. Am. Chem. Soc.* **2005**, *127*, 12647–12656.
(9) Walter, E. D.; Chattopadhyay, M.; Millhauser, G. L. *Biochemistry* **2006**, *45*, 13083–13092.

(10) Burns, C. S.; Aronoff-Spencer, E.; Legname, G.; Prusiner, S. B.; Antholine, W. E.; Gerfen, G. J.; Peisach, J.; Millhauser, G. L. *Biochemistry* **2003**, *42*, 6794–6803.
(11) Jones, C. E.; Abdelraheim, S. R.; Brown, D. R.; Viles, J. H. *J. Biol. Chem.* **2004**, *279*, 32018–32027.
(12) Belosi, B.; Gaggelli, E.; Guerrini, R.; Kozlowski, H.; Luczkowski, M.; Mancini, F. M.; Remelli, M.; Valensin, D.; Valensin, G. *ChemBioChem* **2004**, *5*, 349–359.
(13) Gaggelli, E.; Bernardi, F.; Molteni, E.; Pogni, R.; Valensin, D.; Valensin, G.; Remelli, M.; Luczkowski, M.; Kozlowski, H. *J. Am. Chem. Soc.* **2005**, *127*, 996–1006.
(14) Kozlowski, H.; Janicka-Klos, A.; Stanczak, P.; Valensin, D.; Valensin, G.; Kulon, K. *Coord. Chem. Rev.* **2008**, *252*, 1069–1078.
(15) Brown, D. R.; Wong, B.-S.; Hafiz, F.; Clive, C.; Haswell, S. J.; Jones, I. M. *Biochem. J.* **1999**, *344*, 1–5.
(16) Rachidi, W.; Vilette, D.; Guiraud, P.; Arlotto, M.; Riondel, J.; Laude, H.; Lehmann, S.; Favier, A. *J. Biol. Chem.* **2003**, *278*, 9064–9072.
(17) Pushie, M. J.; Rauk, A. *J. Biol. Inorg. Chem.* **2003**, *8*, 53–65.
(18) Riihimaki, E.-S.; Kloo, L. *Inorg. Chem.* **2006**, *45*, 8509–8516.
(19) Bruschi, M.; Gioia, L. D.; Mitric, R.; V., B.-K.; Fantucci, P. *Phys. Chem. Chem. Phys.* **2008**, *10*, 4573–4583.
(20) Ames, W. M.; Larsen, S. C. *J. Biol. Inorg. Chem.* **2009**, *14*, 547–557.
(21) Pandey, K. K.; Snyder, J. P.; Liotta, D. C.; Musaev, D. G. *J. Phys. Chem. B* **2010**, *114*, 1127–1135.
(22) Furlan, S.; Penna, G.; Guerrieri, F.; Morante, S.; Rossi, G. C. *J. Biol. Inorg. Chem.* **2007**, *12*, 571–583.
(23) Marino, T.; Russo, N.; Toscano, M. *J. Phys. Chem. B* **2007**, *111*, 635–640.
(24) Riihimaki, E.-S.; Martinez, J. M.; Kloo, L. *J. Phys. Chem. B* **2007**, *111*, 10529–10537.
(25) Redecke, L.; Meyer-Klaucke, W.; Koker, M.; Clos, J.; Georgieva, D.; Genov, N.; Echner, H.; Kalbacher, H.; Perbandt, M.; Bredehorst, R.; Voelter, W.; Betzel, C. *J. Biol. Chem.* **2005**, *280*, 13987–13992.
(26) Ling, Y.; Mills, C.; Weber, R.; Yang, L.; Zhang, Y. *J. Am. Chem. Soc.* **2010**, *132*, 1583–1591.
(27) McMahon, M. T.; deDios, A. C.; Godbout, N.; Salzmann, R.; Laws, D. D.; Le, H. B.; Havlin, R. H.; Oldfield, E. *J. Am. Chem. Soc.* **1998**, *120*, 4784–4797.
(28) Zhang, Y.; Gossman, W.; Oldfield, E. *J. Am. Chem. Soc.* **2003**, *125*, 16387–16396.
(29) Zhang, Y.; Oldfield, E. *J. Am. Chem. Soc.* **2004**, *126*, 9494–9495.
(30) Zhang, Y.; Oldfield, E. *J. Am. Chem. Soc.* **2004**, *126*, 4470–4471.
(31) Mao, J. H.; Mukherjee, S.; Zhang, Y.; Cao, R.; Sanders, J. M.; Song, Y. C.; Zhang, Y. H.; Meints, G. A.; Gao, Y. G.; Mukkamala, D.; Hudock, M. P.; Oldfield, E. *J. Am. Chem. Soc.* **2006**, *128*, 14485–14497.
(32) Zhang, Y.; Oldfield, E. *J. Am. Chem. Soc.* **2008**, *130*, 3814–3823.
(33) Ling, Y.; Zhang, Y. Deciphering Structural Fingerprints for Metalloproteins with Quantum Chemical Calculations. In *Annual Reports in Computational Chemistry*; Wheeler, R. A., Ed.; Elsevier: New York, 2010; Vol. 6, pp 65−77.
(34) Ling, Y.; Davidson, V. L.; Zhang, Y. *J. Phys. Chem. Lett.* **2010**, *1*, 2936–2939.
(35) Shewmaker, F.; Wickner, R. B.; Tycko, R. *Proc. Natl. Acad. Sci. U.S.A.* **2006**, *103*, 19754–19759.
(36) Wasmer, C.; Lange, A.; Van Melckebeke, H.; Siemer, A. B.; Riek, R.; Meier, B. H. *Science* **2008**, *319*, 1523–1526.
(37) Zhang, Y.; Sun, H. H.; Oldfield, E. *J. Am. Chem. Soc.* **2005**, *127*, 3652–3653.
(38) Kervern, G.; Pintacuda, G.; Zhang, Y.; Oldfield, E.; Roukoss, C.; Kuntz, E.; Herdtweck, E.; Basset, J. M.; Cadars, S.; Lesage, A.; Coperet, C.; Emsley, L. *J. Am. Chem. Soc.* **2006**, *128*, 13545–13552.
(39) Ling, Y.; Zhang, Y. *J. Am. Chem. Soc.* **2009**, *131*, 6386–6388.
(40) Mao, J. H.; Zhang, Y.; Oldfield, E. *J. Am. Chem. Soc.* **2002**, *124*, 13911–13920.
(41) Dudev, T.; Lim, C. *J. Phys. Chem. B* **2009**, *113*, 11754–11764.
(42) Adamo, C.; Barone, V. *J. Chem. Phys.* **1998**, *108*, 664–675.
(43) Perdew, J. P.; Burke, K.; Wang, Y. *Phys. Rev. B* **1996**, *54*, 16533–16539.
(44) Zhang, Y.; Guo, Z. J.; You, X. Z. *J. Am. Chem. Soc.* **2001**, *123*, 9378–9387.
(45) Zhang, Y.; Lewis, J. C.; Bergman, R. G.; Ellman, J. A.; Oldfield, E. *Organometallics* **2006**, *25*, 3515–3519.
(46) Balof, S. L.; Yu, B.; Lowe, A. B.; Ling, Y.; Zhang, Y.; Schanz, H. J. *Eur. J. Inorg. Chem.* **2009**, 1717–1722.
(47) Stevenson, S.; Ling, Y.; Coumbe, C. E.; Mackey, M. A.; Confait, B. S.; Phillips, J. P.; Dorn, H. C.; Zhang, Y. *J. Am. Chem. Soc.* **2009**, *131*, 17780–17782.
(48) Becke, A. D. *Phys. Rev. A* **1988**, *38*, 3098–3100.
(49) Lee, C.; Yang, W.; Parr, R. G. *Phys. Rev. B* **1988**, *37*, 785–789.
(50) Hohenberg, P.; Kohn, W. *Phys. Rev. B* **1964**, *136*, 864–871.
(51) Vosko, S. H.; Wilk, L.; Nusair, M. *Can. J. Phys.* **1980**, *58*, 1200–1211.
(52) Becke, A. D. *J. Chem. Phys.* **1993**, *98*, 5648–5652.
(53) Wachters, A. J. *J. Chem. Phys.* **1970**, *52*, 1033–1036.
(54) Frisch, M. J.; Trucks, G. W.; Schlegel, H. B.; Scuseria, G. E.; Robb, M. A.; Cheeseman, J. R.; Montgomery, Jr., J. A.; Vreven, T.; Kudin, K. N.; Burant, J. C.; Millam, J. M.; Iyengar, S. S.; Tomasi, J.; Barone, V.; Mennucci, B.; Cossi, M.; Scalmani, G.; Rega, N.; Petersson, G. A.; Nakatsuji, H.; Hada, M.; Ehara, M.; Toyota, K.; Fukuda, R.; Hasegawa, J.; Ishida, M.; Nakajima, T.; Honda, Y.; Kitao, O.; Nakai, H.; Klene, M.; Li, X.; Knox, J. E.; Hratchian, H. P.; Cross, J. B.; Bakken, V.; Adamo, C.; Jaramillo, J.; Gomperts, R.; Stratmann, R. E.;Yazyev, O.; Austin, A. J.; Cammi, R.; Pomelli, C.; Ochterski, J. W.; Ayala, P. Y.; Morokuma, K.; Voth, G. A.; Salvador, P.; Dannenberg, J. J.; Zakrzewski, V. G.; Dapprich, S.; Daniels, A. D.; Strain, M. C.; Farkas, O.; Malick, D. K.; Rabuck, A. D.; Raghavachari, K.; Foresman, J. B.; Ortiz, J. V.; Cui, Q.; Baboul, A. G.; Clifford, S.; Cioslowski, J.; Stefanov, B. B.; Liu, G.; Liashenko, A.; Piskorz, P.; Komaromi, I.; Martin, R. L.; Fox, D. J.; Keith, T.; Al-Laham, M. A.; Peng, C. Y.; Nanayakkara, A.; Challacombe, M.; Gill, P. M. W.; Johnson, B.; Chen, W.; Wong, M. W.; Gonzalez, C.; Pople, J. A. *Gaussian 03, Revision D.01*; Gaussian, Inc.: Wallingford, CT, 2004.